Journal of Sol-Gel Science and Technology (2020) 95:265–275
https://doi.org/10.1007/s10971-020-05318-8

ORIGINAL PAPER: FUNCTIONAL COATINGS, THIN FILMS AND MEMBRANES (INCLUDING DEPOSITION TECHNIQUES)

Formaldehyde detection using Sn doped ZnO thin film

Syafiqah Ishak[1] · Shazlina Johari[1] · Muhammad Mahyiddin Ramli[1]

Received: 18 February 2020 / Accepted: 13 May 2020 / Published online: 24 May 2020

Abstract

This work presents an approach for formaldehyde detection using Sn doped ZnO thin film. The concentration of Sn dopant varies at 0.5at%, 1.0at% and 1.5at%. XRD results show that the thin film possessed a crystallite structure with the highest peak at 002. The crystallite size of undoped, 0.5at%, 1.0at% and 1.5at% Sn doped ZnO thin film are 10.09 nm, 33.36 nm, 8.736 nm and 9.31 nm, respectively. Surface roughness obtained from AFM was 16.9 nm, 10.19 nm, 5.48 nm and 8.57 nm for undoped 0.5at%, 1.0at% and 1.5at% Sn doped ZnO thin film, respectively. The optimal sensitivity is acquired when 1.0at% Sn doped ZnO thin film is used for the detection of 3.4 ppb formaldehyde, where the sensing performance is 92%; while the sensing performance of undoped thin film is only 50%. The response time for undoped and 1.0at% Sn doped ZnO thin film is 10-8 s and 4-10 s, while the recovery time is 38-207 s and 15-34 s, respectively. The 1.0at% Sn doped ZnO thin film also demonstrates a good response in formaldehyde sensing, which was measured for nine consecutive days, where the sensing performance was over 90%.

Graphical Abstract

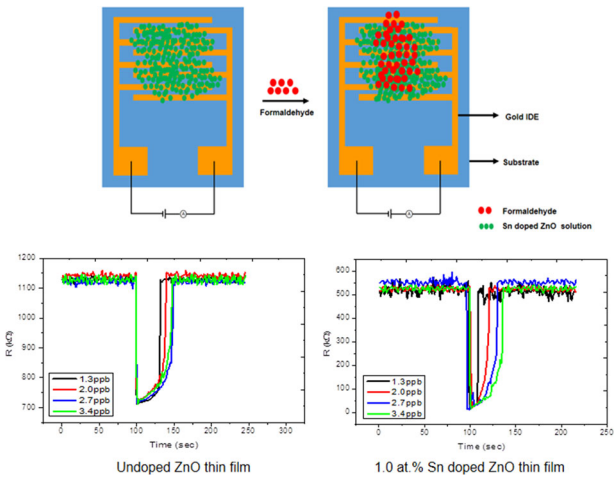

Keywords Sol–gel · Spin Coating · Sn doped ZnO thin film · Formaldehyde sensor

✉ Shazlina Johari
shazlinajohari@unimap.edu.my

[1] School of Microelectronic Engineering, Universiti Malaysia Perlis, Pauh Putra Campus, Arau, Perlis 02600, Malaysia

Highlights

- Sn doped ZnO thin film with various concentrations (0.5 at.%, 1.0 at.% and 1.5 at.%) on an interdigitated electrode (IDE) was prepared by using the sol gel method.
- Sn doping increased the gas sensitivity due an excess of free electrons, whereby 1.0 at.% Sn doped was the best sensor for detecting formaldehyde, with a response of up to 92%.
- A 1.0 at.% Sn doped ZnO thin film can maintain the sensitivity for over 65% for 9 consecutive days, compared with an undoped ZnO thin film.

1 Introduction

Formaldehyde is an organic compound that is often used in various products such as paper, paint, medicine, cosmetics, glue, and antiseptics. However, extensive exposure of formaldehyde can negatively affect human health. The effect of the over exposure of formaldehyde involves irritation of the nose, eyes and throat. This can potentially lead to leukaemia and nasopharyngeal cancer [1]. Therefore, it is imperative to monitor and control the presence of formaldehyde in the environment.

There are several existing methods of formaldehyde detection such as optical detection devices and gas chromatography-mass spectrometry (GC-MS) [2]. However, although the GC-MS method has better sensitivity, the high cost and heavy equipment is not favoured for in-field measurement [3, 4]. Optical sensors tend to be large and expansive when used, even though they are less time consuming [5, 6].

Gas sensors based on metal oxides such as tin dioxide (SnO_2) [7, 8], titanium dioxide (TiO_2) [9, 10], and zinc oxide (ZnO) [11, 12] have played a crucial role in this area, attributable to their good sensing responses and the easy modification of their electrical characteristics. Gas sensors based on thin film ZnO are particularly favoured for sensing applications, primarily because of their tuneable surface morphology, large surface-to-volume ratio, and excellent stability due to better crystallinity [13]. Typically, metal oxide semiconductor material is deposited in the form of thin or thick film, and is used as an active layer for gas sensing devices. For the detection of toxic gases, semiconductors based chemiresistor sensor are mostly investigated, due to their low cost and simplicity. The principle of chemi-resistivity is based on the change of electrical resistance that results from the interaction of metal oxide semiconductors and the targeted gas [14]. This type of sensor has relatively high sensitivity, low cost, short response time and applicability in portable instruments.

There are various methods that can be applied in order to produce Sn doped ZnO thin film such as spray pyrolysis, pulse laser deposition [15], electron beam evaporation [16], and magnetron sputtering [17]. Spray pyrolysis can easily be performed, since no high temperature is required, and the film's quality depends on the size of the droplet and nozzle used [18]. However, as the spray method is conducted in open air, sulphide oxidation may occur, which could lead to the cluttering of the spray nozzle after multiple uses. Pulse laser deposition is also used to produce thin film, as it can control the growth rate of the film. However, if large kinetic energy is used, re-sputtering could occur, and subsequently affect the growth of the thin film [19].

Meanwhile, electron beam evaporation has a high film deposition rate and high purity form. However, it is difficult to be controlled and to enhance the step coverage, and the x-ray by the electron beam evaporation can be harmful if it is misused [20]. Magnetron sputtering, which involves a strong electric and magnetic field, can also be used. It has better film quality and can be used for a large target area [21]. However, the substrate can be damaged due to high ion bombardment by plasma, and it is difficult to distribute the solution uniformly, especially with a complex shape. Futhermore, it is also challenging to produce thick film coating due to high residual stress levels.

In this paper, Sn doped ZnO interdigitated electrode (IDE) structure is introduced to detect formaldehyde at a low temperature using the sol-gel method. The operating temperatures used in this work are 130 °C, 150 °C, 170 °C, and 190 °C, with various doping concentrations of 0.5 at%, 1.0 at%, and 1.5 at%. The doped IDE structure is used as a sensing device to detect formaldehyde. The dopant used is Sn ions, because when Sn becomes Sn^{4+} after being replaced for Zn^{2+} in the ZnO structure, it has two free electron remaining [14]. This is important for electron conduction activity. According to Yung [22], doping plays a significant role in optical properties, as it can modify the characteristics of ZnO thin film by affecting the grain size and vibrational structure of the thin film. Due to the radius difference between Sn^{4+} and Zn^{2+} being about 30% ($Zn^{2+} = 0.74$ Å and $Sn^{4+} = 0.69$ Å), a limited solid solution could be created. The sensing device is made up of a glass substrate (22.8×7.6 mm) deposited with a gold interdigitated electrode (IDE) obtained from DropSens. The reason for using IDE is because better electrical conductivity can be achieved when the formaldehyde is attached to the device. IDE technology with different gap sizes has been proven to be sensitive, can be used with a low volume of samples, and at the same time, enhances the detection limit

while providing a quick response for sensor application, as reported by Ajili et al. [23, 24].

2 Experimental procedure

2.1 Sol–gel process

The precursor for colloids/nanoparticles in the sol-gel process consists of a metal or metalloid element [25]. Zinc acetate is an organic compound that is widely used in sol-gel. The sol-gel process can be classified into three types of growth, which are solution growth, hydrothermal and template-based growth [25]. The hydrolysis and condensation method takes place in the solution growth process. First, zinc acetate dehydrate dissociates into zinc monoacetate and acetate ions in the alcoholic solution [26]. Then, the acetate ions and water are adsorbed on the substrate, and when zinc monoacetate is hydrolysed, zinc oxide and acetic acid are produced. Since the drying temperature is higher (150 ˚C) than boiling point (118 ˚C), the acid is evaporated [26]. The condensation process occurs in an alkaline solution where ethanolamine is provided [26]. Ethanolamine is a bidentate ligand, and works as a chelating and stabilizing ligand that prevents the precipitation of ZnOH and encourages the bridge between two zinc atoms [26]. Once monoacetate is formed, it reacts with OH/NH_2 from ethanolamine [26].

2.2 Sol-gel synthesis of ZnO

In this work, zinc acetate dehydrate ($ZnC_4H_6O_4$) and tin chloride pentahydrate ($Cl_4H_5O_5Sn$) were mixed together and dissolved in 2-methoxyethanol ($CH_3OCH_2CH_2OH$). The chemicals were purchased from Sigma Aldrich. The concentrations of tin chloride pentahydrate ($Cl_4H_5O_5Sn$) used in the mixture were 0.5 at.%, 1.0 at.% and 1.5 at.%. The precursor was stirred for 1 hour at 80 ˚C. Then, ethanolamine (C_2H_7NO) as a stabilizer was added drop by drop until the solutions became homogeneous, with a molar ratio of 1:1. After that, the precursor was aged for 24 h at room temperature.

2.3 Spin-coating deposition

The prepared precursor was then deposited on an Au interdigitated electrode by using the spin coating method. The speed used was 500 rpm for 40 s. The solvent evaporation, followed by condensation reactions, resulted in the deposition of solid film on the Au interdigitated electrode substrate. Then, the substrate was soft baked for 10 min at 150 ˚C, to remove any organic residue. The process was repeated six times to obtain the desired thickness. After that, the substrate was annealed for 5 hours at 500 ˚C in a furnace.

2.4 Characterization of the thin film

The structure properties were analysed by using a Bruker advanced diffractometer with CuKα radiation (λ = 1.5406 Å) as the x-ray source, XRD. Surface morphological characteristics were investigated by a JEOL SEM operated at 15k eV and AFM. The electrical resistance was measured by the two probe method using an E4980A Precision LCR Metre.

2.5 Chemiresistivity and gas sensor set-up

Figure 1 shows the schematic diagram of the ZnO-based chemiresistive gas sensor used in this work. The prepared precursor was dropped between fingers of Au interdigitated electrode (IDE) of the gas sensor, and then annealed at 500 ˚C for 5 h.

The formaldehyde sensing measurement was conducted based on the setup illustrated in Fig. 2. The device was placed in a closed chamber (25 cm × 15 cm × 25 cm) on a hotplate (1 cm in diameter) at the temperatures of 130 °C, 150 °C, 170 °C and 190 °C. Initially, the resistance of the device was recorded for five minutes to ensure the device is stable, before formaldehyde was introduced. Then, a predefined amount of formaldehyde was injected by using

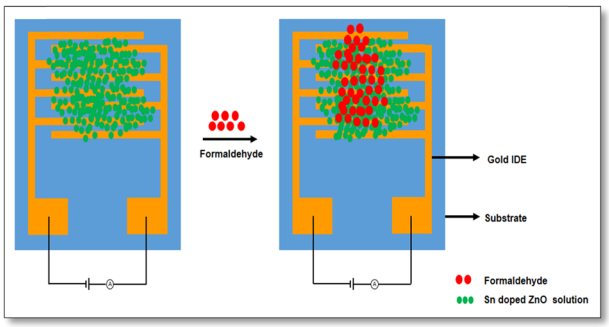

Fig. 1 A schematic diagram of ZnO based chemiresistivity gas sensor

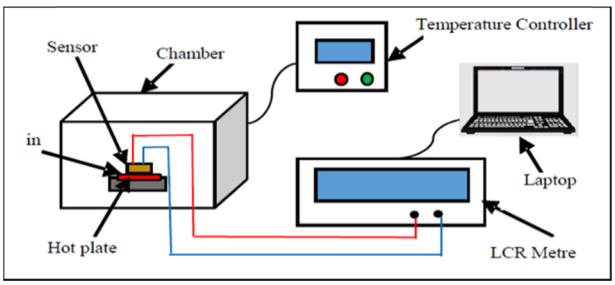

Fig. 2 Schematic diagram of the test chamber

micropipette into the chamber, while the resistance value of the device was recorded. Since the formaldehyde used in this work is in liquid form, Eq. 1 is used to convert the amount of injected liquid into a gas concentration of ppb [27]:

$$C = \left[\frac{V_L \times D_L \times T}{M_L \times V_A}\right] \times 8.2 \times 10^4 \times 1000 \quad (1)$$

where C is the concentration in ppb, V_L (μL) is the volume of the formaldehyde, D_L (g ml^{-1}) is the density of the formaldehyde, T (K) is the operating temperature, M_L (g mol^{-1}) is the molar mass of the formaldehyde, and V_A (mL) is the volume of the diluted gas, which is equal to the test chamber. The device took some time to recover to the initial resistance value. Once the resistance reading returned to the initial point, it was assumed that the device fully recovered, and the experiment was repeated for various concentrations of Sn doped ZnO thin film.

3 Results and discussion

3.1 Structural and morphological characteristics

The X-ray diffraction data in Fig. 3 shows that when ZnO thin film is doped with Sn^{4+}, the diffraction peak shifted at a high degree, with respect to 002. This is due to the smaller ionic radius of Sn^{4+} (0.069 nm), compared with the ionic radius of Zn^{2+} (0.074 nm), which leads to the replacement of Zn [23].

The crystallite size of the thin film is calculated and tabulated in Table 1 based on Bragg's Law equation. The crystallite size decreases as the doping increases. However, there exists variations in the crystallite size due to the changes in density of nucleation center, thus resulting in the decrease in the crystallite size when compressive stress occurs. The crystallite size increased to the original size when the crystal structure underwent tensile stress. This explains why, at a doping concentration of 0.5at% Sn, the crystallite size was slightly higher, and decreased when further doping was introduced. Similar cases of change in crystallite size with doping presence has also been reported in the related literature [28].

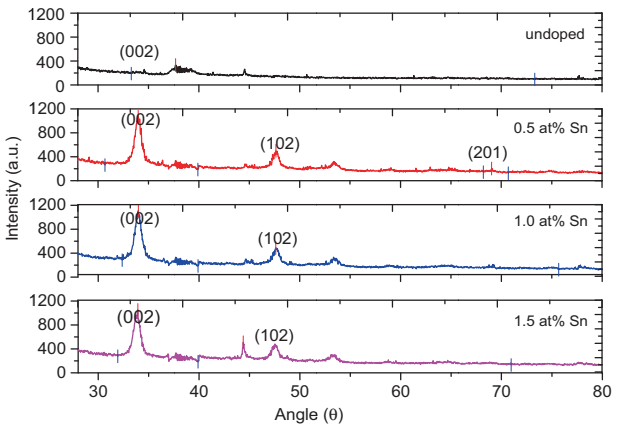

Fig. 3 X-ray diffraction pattern of undoped and Sn doped ZnO thin film annealed at 500 °C for 5 h

The XRD diffraction peak for undoped and doped ZnO thin film in Table 1 is compared with JCPDS No.: 05-0664, and shows a stable hexagonal wurtzite structure. The crystallite size, d, is calculated by using the following equation:

$$D = \frac{0.9\lambda}{\beta \cos\theta} \quad (2)$$

where λ is the x-ray wavelength, D is the crystallite size, β is the broadening of diffraction line in radian and θ is the angle of incidence. As shown in the table, the crystallite size decreases when doping is present. This situation occurs because there is incorporation of tin into the lattice [28].

Figure 4a shows the SEM images of undoped ZnO thin film after annealing at 500 °C. The image shows that the samples are densely packed with non-spherical particles of a hexagonal wurtzite structure. The ZnO structure becomes a hexagonal nanodisc as the annealing temperature and time is high [29]. When the Sn^{4+} dopant is introduced at 1.5 at. %, it can be observed that it is wrapped around the ZnO particle, as shown in Fig. 4b [30]. Further proof of the presence of Sn in ZnO is shown in XRD at the peak of 40–45° (220) at 1.5 at.% [31]. In terms of surface roughness, Fig. 5 shows the relation between the surface roughness and the size of the grain for different doping concentrations. The surface roughness for undoped is the lowest at 5.48 nm, and the highest surface roughness is recorded for 1.5 at.% Sn doped ZnO thin film is 16.7 nm. This trend shows that when the dopant concentration increases, the average grain size decreases. This situation was also reported by Zahari [20]. The thickness of the thin film that was measured using a stylus profilometer is about 150–160 nm. Therefore, as the film thickness is below 200 nm, only a small part of the grain has changed, whereas the in-plane grain size does not differ much.

When the grain size decreases, the value of the surface roughness increases, and this situation occurs because there

Table 1 XRD analysis for undoped and doped ZnO thin film

ZnO Thin Film	Position (2θ)	d spacing observed (Å)	*d* spacing JCPDS (Å)	hkl	Crystallite Size, *D* (nm)
Undoped	34.5	2.592	2.602	002	10.1
0.5 at.%	33.9	2.634	2.602	002	33.4
1.0 at.%	33.7	2.650	2.602	002	8.7
1.5 at.%	33.7	2.650	2.602	002	9.3

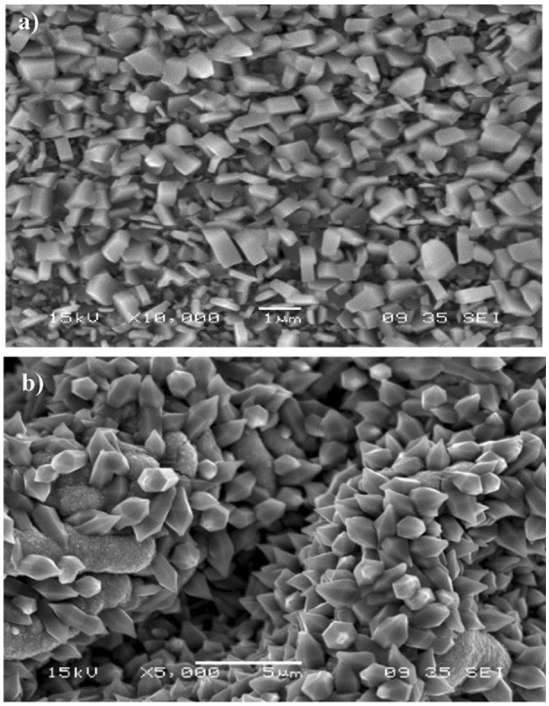

Fig. 4 SEM images of **a** undoped and **b** 1.5 at.% Sn doped ZnO thin film

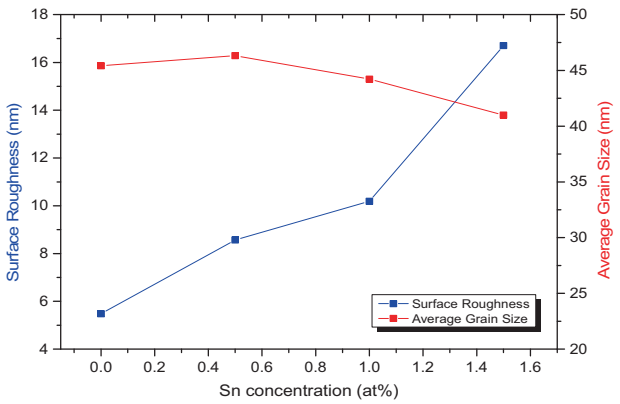

Fig. 5 Surface roughness (RMS), average grain size and crystallite size of undoped and doped ZnO thin film

was substitution of the Sn in the ZnO thin film. The increase of surface roughness favours the adsorption of atmospheric oxygen on the surface, thus increasing the sensing response [32]. It is important to have a smaller grain and crystallite size for good sensing performance. However, as depicted in Table 1, for 0.5 at.% Sn doped, the grain size is higher compared with others. This is probably due to the crystallite overlap caused by agglomeration [33], which alters the surface roughness. Since the grain size of the thin film affects the gas sensitivity [10], it is expected that the small crystallite size in this work will reflect a higher gas sensitivity response.

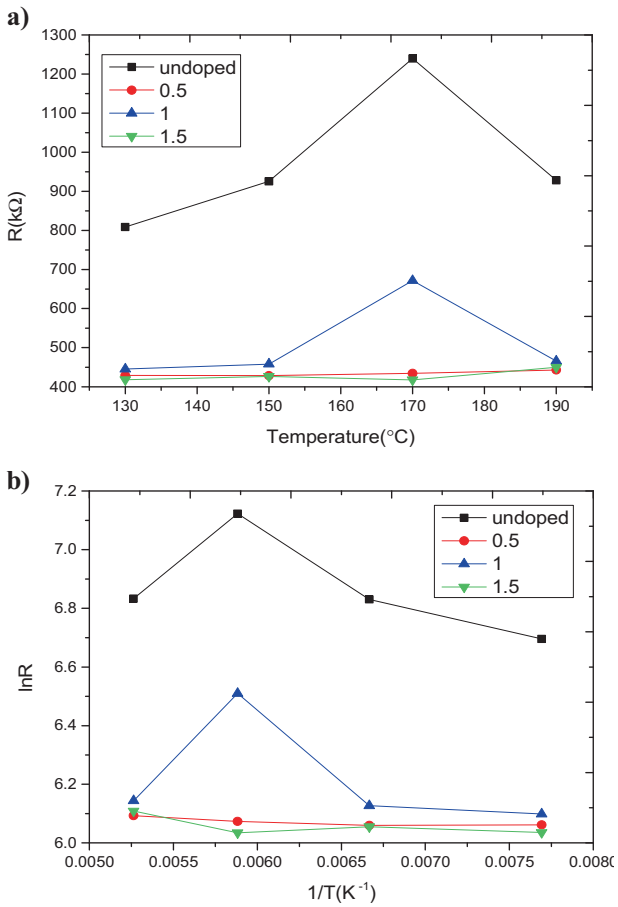

Fig. 6 **a** Electrical resistance as a function of temperature and **b** inverse absolute temperature of the films

3.2 Electrical properties

An Agilent LCR metre was used to measure the electrical characteristics for undoped and Sn doped ZnO thin films. A dc-two probe method was used to measure the resistivity of the doped and undoped ZnO films. A variety of resistance values that act as a function of temperature and inverse absolute temperature in the range of 130 to 190 °C are shown in Fig. 6. The resistance value for undoped ZnO thin film is higher compare to doped ZnO thin film, due to the contribution of ions from Sn^{4+} on site of Zn^{2+} ions [34]. Two processes occur simultaneously when the temperature is increased, namely, thermal excitation of electrons, and adsorption of electrons. The thermal action of the electrons process is influenced by the oxygen adsorption as the resistance increases to 170 °C for undoped ZnO thin film. However, the oxygen adsorption at the surface of the thin film is dominated by the thermal action of electrons when the temperature increases, which decreases the resistance value [25]. This situation occurs when the temperature exceeds 180 °C, which decreases the resistance further. This trend is in line with prior works [35, 36].

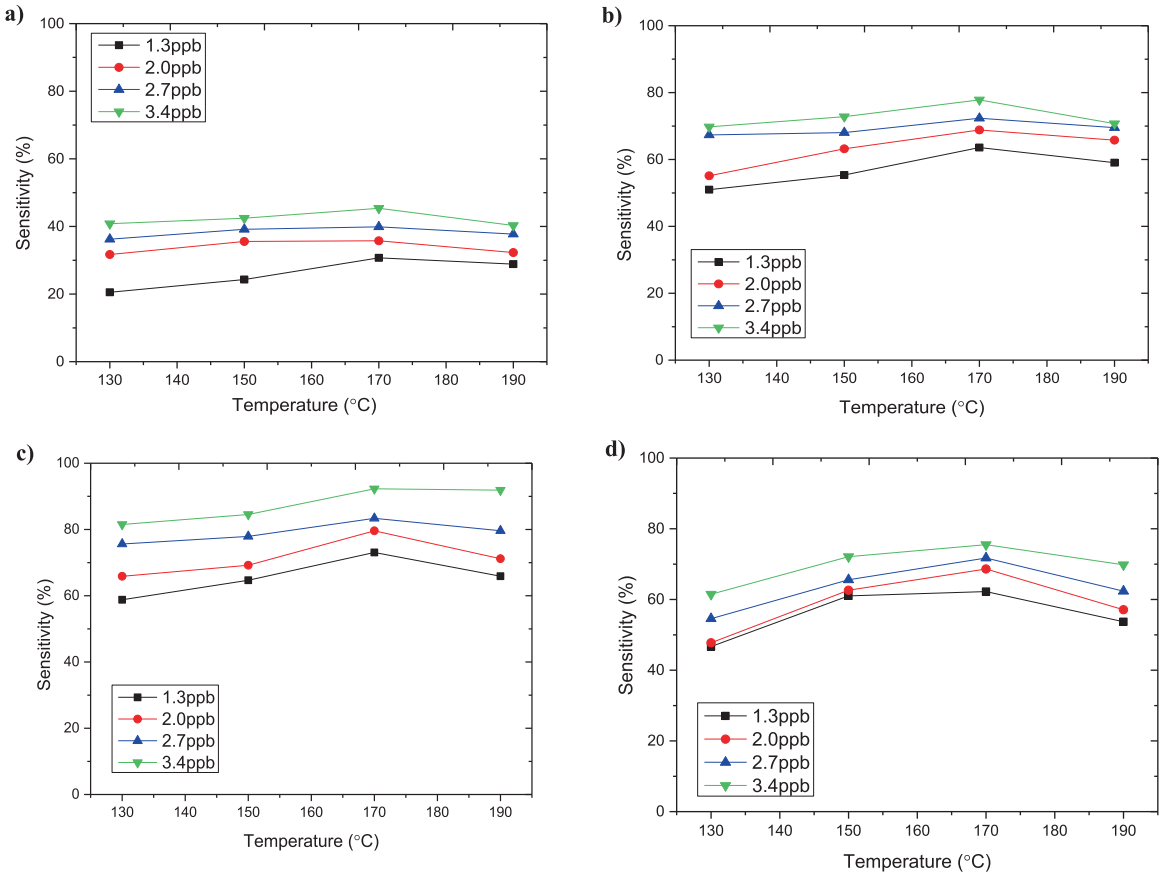

Fig. 7 Sensitivity response of formaldehyde in various concentrations as a function of temperature at 130 °C, 150 °C, 170 °C and 190 °C for **a** undoped, **b** 0.5 at.%, **c** 1.0 at.%, and **d** 1.5 at.% Sn doped ZnO thin film

3.3 Formaldehyde sensing analysis

The gas response of formaldehyde is investigated in order to identify the lowest amount of formaldehyde that can be detected. The value of resistance was recorded before and after the presence of formaldehyde, and the sensitivity was calculated by using the following equation:

$$S[\%] = \left[\left(R_a - R_g\right)/R_a\right] \times 100\% \quad (3)$$

where R_a is the resistance before formaldehyde is introduced, and R_g is the resistance after its introduction. The response and recovery time of the undoped and Sn doped ZnO thin film is defined as the time required to achieve 90% when formaldehyde is present, and to reach its baseline when formaldehyde is absent. Figure 7 shows formaldehyde sensitivity response within the temperature range of 130–190 °C. According to the figure, 1.0 at.% Sn doped ZnO thin film exhibits the best sensitivity towards formaldehyde. The best response for doped ZnO thin film is when the operating temperature is at 170 °C, which has high sensitivity for 1.3 ppb, 2.0 ppb, 2.7 ppb and 3.4 ppb of formaldehyde.

Hence, the change in the resistance of the doped ZnO thin film as a function of time with the presence of formaldehyde at this

particular temperature is presented in Figs. 8 and 9. The total response and recovery time of the device is tabulated in Table 2, while the response and recovery time is shown in Figs. 8 and 9 for undoped and 1.0 at.% doped ZnO thin film, respectively.

Based on these figures, 1.0 at.% doped ZnO thin film shows the shortest response and recovery time compared with undoped ZnO thin film. The response and recovery time are longer when the amount of formaldehyde solution is increased.

Figure 10 shows the response stability of undoped and 1.0 at.% doped ZnO for 1.3 ppb, 2.0 ppb, 2.7 ppb and 3.4 ppb formaldehyde concentration at a temperature of 170 °C. The experiment was conducted continuously for nine days for 1.0 at.% doped ZnO thin film. The gas sensing response time was recorded throughout nine continuous days. It can be seen that the sensor is stable, as the response recorded for undoped and 1.0 at.% Sn doped ZnO thin film shows fluctuations of 3 and 2% only, as compared with the work done

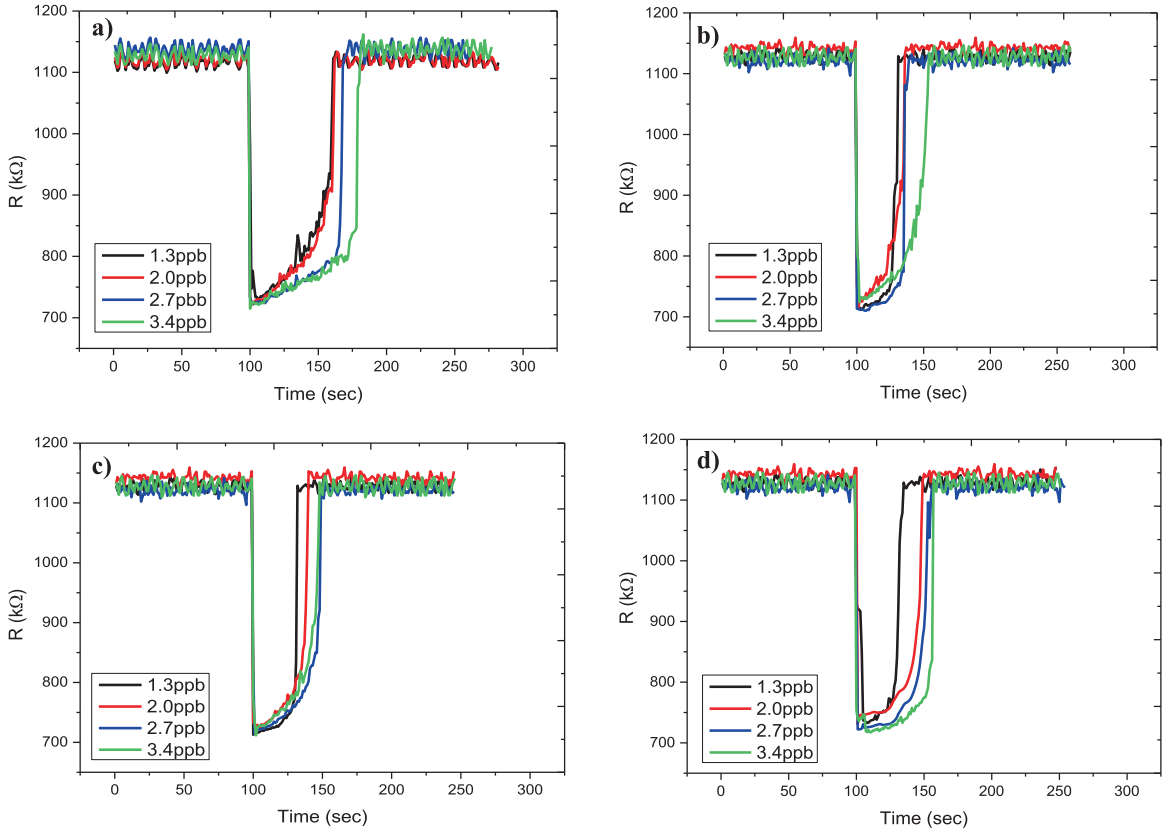

Fig. 8 Response and recovery time of formaldehyde at a temperature of **a** 130 °C, **b** 150 °C, **c** 170 °C, and **d** 190 °C for undoped ZnO thin film

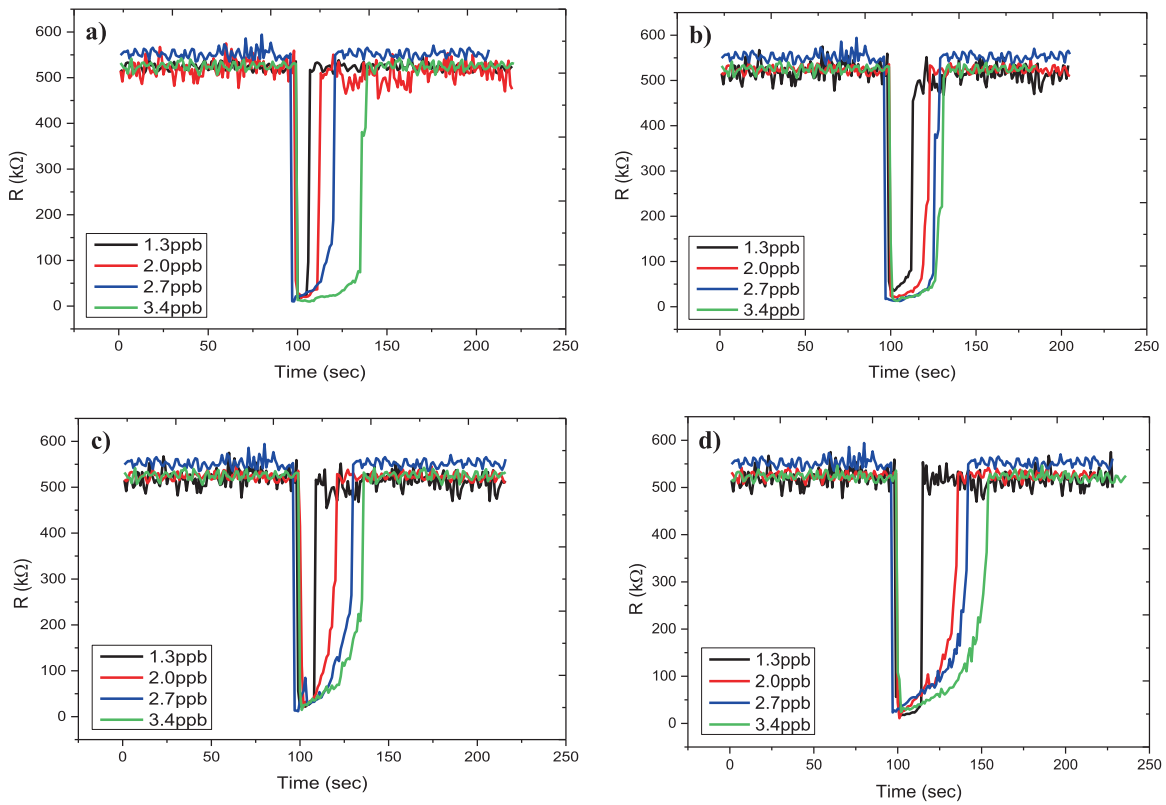

Fig. 9 Response and recovery time of formaldehyde at a temperature of **a** 130 °C, **b** 150 °C, **c** 170 °C, and **d** 190 °C for 1.0 at.% doped ZnO thin film

by Prajapati [32], where it shows a fluctuation of 6% at an operating temperature 275 °C for 9 days.

The sensing mechanism of ZnO is dependent on the surface controlled type. The sensitivity is affected by the active layer grain size, oxygen adsorption, surface state and lattice defects [37]. In order to enhance the sensing response, Sn^{4+} dopants were introduced. Dopants increase the sensing response by altering the resistance of ZnO. According to Bhati [38], dopants can reduce the working temperature of the sensor, enhance the stability and sensitivity, and give a high response towards the targeted gas. This is because, when dopants are introduced, the surface morphology and grain size changes. The grain size of doped ZnO became smaller as the dopant inhibits the crystal growth rate. Thus, this can improve the sensing performance as a small sized particle has a high surface area, hence increasing the chemisorbed oxygen ions.

Table 2 Average total response and recovery time of undoped and 1.0 at.% doped ZnO thin film

Formaldehyde Concentration (ppb)	Temperature (°C)	Undoped	1.0 at.% Sn doped ZnO
1.3	130	60 s	7 s
2.0		61 s	14 s
2.7		67 s	20 s
3.4		80 s	38 s
1.3	150	30 s	12 s
2.0		35 s	22 s
2.7		38 s	28 s
3.4		53 s	30 s
1.3	170	31 s	9 s
2.0		39 s	20 s
2.7		48 s	29 s
3.4		47 s	35 s
1.3	190	34 s	14 s
2.0		48 s	35 s
2.7		55 s	41 s
3.4		57 s	53 s

Oxygen vacancies are also among the factors that affect the effectiveness of a metal oxide semiconductor. Oxygen vacancy acts as an electron donor and a direct adsorption site [39]. In this work, ZnO is n –type material, and the doping of Sn^{4+} increases the conductivity by enhancing the electron density [40]. This is due to the Sn^{4+} annihilating the variation of oxygen species. Sn may be incorporated with a ZnO lattice, as their ionic radii is about the same (0.074 nm for Zn^{2+} and 0.069 nm for Sn^{4+}). In the ZnO lattice, Sn remains as a defect with a negative charge. The conductivity is increased due to the oxygen vacancy, and ZnO is associated with an oxygen deficiency. The Sn donor is ionized and doubly ionized in the oxygen vacancy in the ZnO material. The Fermi level should be close to the conduction band in the n-type semiconductor. Hence, being doped with Sn (donor) will contribute more electrons to the reaction, as the majority carriers are electrons, and the minority carriers are the holes.

Besides this, the detection of the ZnO based gas sensor is obtained from the variation in electrical resistivity. Since the annealing temperature used is high, which is at 500 °C, the ZnO resistivity also increases because of the chemisorption of oxygen at the grain boundaries, thus encouraging the formation of the extrinsic trap localized at the boundaries. As such, this trapped electron creates a potential barrier by producing a depletion region to the grain boundaries. This situation causes the resistivity to increase as the mobility carrier decreases.

Oxygen molecules in the atmosphere were absorbed by the surface of the sample combined with an electron in the

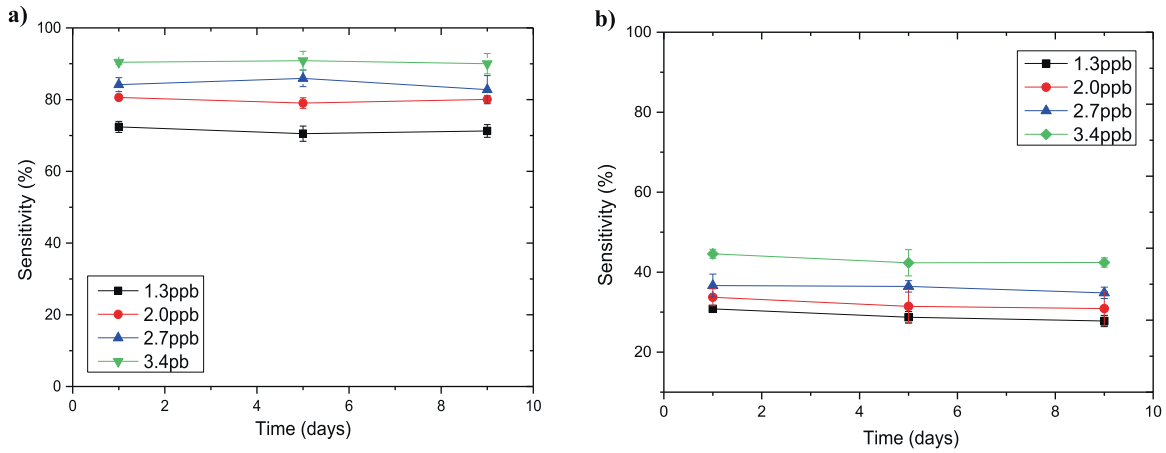

Fig. 10 Response stability of **a** 1.0 at.% doped and **b** undoped ZnO thin film towards formaldehyde at a temperature of 170 °C as a function of time in days

Table 3 Previous works on low level of formaldehyde detection as compared with this work

Sensing element	Method	Operating Temp. °C	Minimum Formaldehyde detection/ppm	Ref
1.0at% Sn doped ZnO thin film	Sol-gel	170	0.001	This work
ZnO nano/microrods	Hydrothermal	400	0.18	[42]
ZnO nanopowder	Microwave	210	0.001	[43]
SnO_2-NiO, microplate	Co-precipitation	300	0.06	[44]
1 mol% Pd-SnO_2 film	Sol-gel	250	0.03	[45]
NiO-SnO_2 nanofibres	Electrospinning	200	0.08	[46]
Pd-SnO_2 fibre	Solvothermal	190	0.05	[47]

conduction band and become ionized, then become absorbed as $2O^-$ (ads). The space charge layer or depletion layer occurs because of the electron transfer between the oxygen molecules and the surface of the ZnO thin film. This region has insufficient carriers because the electrons are trapped by chemisorbed oxygen. This situation causes the conductance of the material to decrease significantly. This shows that electrical conductivity is strongly dependent on the surface state resulting from the molecular adsorption in the region.

The high surface area typically favors high adsorption–desorption sites, thus increasing sensitivity. When the metal oxide surface adsorb the atmospheric oxygen, different oxygen species are formed, depending on the operating temperature used, as shown in Eqs. 4a–4c. However, when there is formaldehyde present, the conductivity of the metal oxide semiconductor changes, thus changing the gas sensitivity as well. When undoped and Sn doped ZnO thin film are introduced with a reducing gas such as formaldehyde, it releases electrons into the conduction band by reacting with the oxygen chemisorbed semiconductor surface. This situation reduces the O_2^- and O^- ions, increases the amount of electrons in the conduction band [41], and also increases the electrical conductivity of the undoped and Sn doped ZnO thin film.

$$O_2(\text{air}) \leftrightarrow O_2(\text{ads}) \tag{4a}$$

$$O_2(\text{ads}) + e^- \leftrightarrow O_{2^-}(\text{ads}) \tag{4b}$$

$$O_2(\text{ads}) + e^- \leftrightarrow 2O^-(\text{ads}) \tag{4c}$$

At first, the atmospheric oxygen gain electron from ZnO and forms $2O_2^-$. It is also well known that the sensing response depends on the number of $2O_2^-$. Formaldehyde then reacts with $2O_2^-$, and the electron is released back to the conduction band, as shown in below equation:

$$HCHO + 2O_2^- \leftrightarrow HCHO + 2O_2 + 2e^- \tag{5}$$

Apart from this, Prajapati [31] described another mechanism of formaldehyde where water and carbon dioxide are formed besides the electron. When formaldehyde is present, the reaction shown in Eq. 6 takes place, and the electron returns to the conduction band.

$$HCHO + O_2^- \leftrightarrow CO_2 + H_2O + e^- \tag{6}$$

The high operating temperature can stimulate the oxidation of formaldehyde, and donates the electron to ZnO. However, as the temperature is continuously increasing, the sensitivity drops because the adsorb oxygen is desorbed from the metal oxide surface.

As shown in Table 3, most of the devices in previous works operate at a higher temperature compared with this work, where it has been found that the optimum operating temperature based on the sensing performance is 170 °C. A low temperature leads to low energy consumption. In terms of the device preparation method, we chose the sol-gel method due to its simplicity, as opposed to other available methods.

4 Conclusion

This paper investigated undoped and Sn^{4+} doped ZnO thin film deposited on Au IDE prepared by sol-gel method for the purpose of formaldehyde sensing. It was found that the use of Sn^{4+} dopant improved the sensitivity and recovery of formaldehyde sensing. The surface roughness of the thin film increased when Sn^{4+} dopant was added, but lowered the size of the grain as more dopant was added. The electrical properties demonstrate that the undoped ZnO thin film has a higher resistance compared with doped ZnO thin film. The most sensitive device is 1.0 at% doped ZnO thin film, as it shows the highest sensitivity response of over 65% towards 1.3 ppb, 2.0 ppb, 2.7 ppb and 3.4 ppb of formadehyde, at 170 °C.

Compliance with ethical standards

Conflict of interest The authors declare that they have no conflict of interest.

References

1. Golden R (2011) Identifying an indoor air exposure limit for formaldehyde considering both irritation and cancer hazards. Crit Rev Toxicol 41:672–721
2. Bagheri H, Ghambarian M, Salemi A, Es-Haghi A (2009) Trace determination of free formaldehyde in DTP and DT vaccines and diphtheria–tetanus antigen by single drop microextraction and gas chromatography–mass spectrometry. J Pharm Biomed Anal 50:287–292
3. Hopkins JR, Still T, Al-Haider S, Fisher IR, Lewis AC, Seakins PW (2003) A simplified apparatus for ambient formaldehyde detection via GC-pHID. Atmos Environ 37:2557–65
4. Wang YH, Chia YL, Che HL, Lung MF (2008) Enhanced sensing characteristics in MEMS-based formaldehyde gas sensors. Microsyst Technol 14:995–1000
5. Levin JO, Andersson K, Lindahl R, Nilsson CA (1985) Determination of sub-part-per-million levels of formaldehyde in air using active or passive sampling on 2,4-dinitrophenylhydrazine-coated glass fiber filters and high-performance liquid chromatography. Anal Chem 57:1032–35
6. Friedfeld S, Fraser M, Lancaster D, Leleux D, Rehle D, Tittel F (2000) Field intercomparison of a novel optical sensor for formaldehyde quantification. Geophys Res Lett 7:2093–96
7. Kim EK, Lee HY, Park J, Park SJ, Kwak JH, Moon SE, Maeng S, Park KH (2004) Fabrication and atmospheric-pressure-dependent electrical properties of a ZnO nanowire device. J Korean Phys Soc 51:170–173
8. Dilonardo E, Penza M, Alvisi M, Di Franco C, Palmisano F, Torsi L, Cioffi N (2016) Evaluation of gas-sensing properties of ZnO nanostructures electrochemically doped with Au nanophases. NBeilstein Journala Nnotechnology 7:22–31
9. Pisarkiewicz T, Sutor A, Potempa P, Maziarz W, Thust H, Thelemann T (2003) Microsensor based on low temperature cofired ceramics and gas sensitive thin film. Thin Solid Films 436:84–89
10. Rothschild A, Komem Y (2004) The effect of grain size on the sensitivity of nanocrystalline metal-oxide gas sensors. J Appl Phys 95:6374–6380
11. Németh Á, Horváth E, Lábadi Z, Fedák L, Bársony I (2007) Single step deposition of different morphology ZnO gas sensing films. Sens Actuators B Chem 127:157–160
12. Kim SD, Kim BJ, Yoon JH, Kim JS (2007) Design, fabrication and characterization of a low-power gas sensor with high sensitivity to CO gas. J Korean Phys Soc 51:2069–2076
13. Katoch A, Abideen ZU, Kim JH, Kim SS, Met (2016) Crystallinity dependent gas-sensing abilities of ZnO hollow fibers. Met Mater Int 22:942–946
14. Fine GF, Cavanagh LM, Afonja A, Binions R (2010) Metal oxide semi-conductor gas sensors in environmental monitoring. Sensors 10:5469–5502
15. Paudel TR, Lambrecht WRL (2006) Phys Rev B 203:1383–1389
16. Agarwal DC, Chauhan RS, Kumar A, Kabiraj D, Singh F, Khan SA, Avasthi DK, Ghatak P, Satyam PV (2006) Synthesis and characterization of ZnO thin film grown by electron beam evaporation. J Appl Phys 99:123105
17. Dave PY, Patel KH, Chauhan KV, Chawla AK, Rawal SK (2016) Examination of Zinc Oxide films prepared by magnetron sputtering. Procedia. Technology 23:328–335
18. Dedova T (2007) Chemical spray pyrolysis deposition of zinc sulfide thin films and zinc oxide nanostructured layers. PhD Thesis, Tallinn University of Technology Estonia
19. Lippert T, Schneider CW (2016) Thin film deposition of functional materials by pulsed laser deposition. https://www.azom.com/article.aspx?ArticleID=5986. Accessed 12 Oct 2018
20. Zahari FF (2012) Electron beam evaporation. https://missinglilo.files.wordpress.com/2012/04/een3106.pdf. Accessed Sept 2017
21. Nair S (2016) Magnetron sputtering. https://www.slideshare.net/SandeepNair41/sputtering-60950269. Accessed Sept 2017
22. Yung KC, Liem H, Choy HS (2009) Enhanced redshift of the optical band gap in Sn doped ZnO free stnding films using the sol-gel method. J Phys D Appl Phys 42:185002
23. Ajili M, Castagné M, Turki NK (2013) Study on the doping effect of Sn-doped ZnO thin films. Superlattices Microstruct 53:213–222
24. Jun LQ, Djaswadi GW, Hawari HF, Zakariya MA (2018) Simulation of interdigitated electrodes (IDEs) geometry using COMSOL multiphysics. International conference on intelligent and advanced system (ICIAS), Kuala Lumpur, pp. 1–6
25. Cauda V, Gazia R, Porro S, Stassi S, Canavese G, Roppolo I, Chiolerio A (2014) Nanostructured ZnO materials:synthesis properties and applications. Handb Nanomater Prop 5:137–177
26. Maia A, Ochoa M, Portugal A, Duraes L (2015) Nanocrystalline ZnO thin films-influence of sol-gel conditions on the underlying chemistry and film microstructure and transparency. Mater Today: Proc 2:49–56
27. Singh V, Hojamberdiev M, Kumar M (2020) Enhanced sensing performance of ZnO nanostructures-based gas sensors. A review. Energy Rep 6:46–62
28. Li Y, Gong J, He G, Deng Y (2012) Enhancement of photoresponse and UV-assisted gas sensing with Au decorated ZnO nanofibers. Mater Chem Phys 134:1172–1178
29. Prajapati CS, Kushwaha A, Sahay PP (2013) Optoelectronics and formaldehyde sensing properties of tin-doped ZnO thin films. Appl Phys A Mater Sci Process 113:651–662
30. Zhang P, Pan G, Zhang B, Zhen J, Sun Y (2014) High sensitivity ethanol gas sensor based on Sn-doped ZnO under visible light irradiation at low temperature. Mater Res 17:4
31. Shaban M, Zayed M, Ahmed MA, Hamdy H (2015) Influence of growth time on the morphology of ZnO nanostructures prepared by low-temperature chemical bath deposition. J Appl Phys 4:35–40
32. Arora N, Jagirdar BR (2014) Au5Sn + AuSn physical mixture to phase pure AuSn and Au5Sn intermetallic nanocrystals with tailored morphology: digestive ripening assisted approach. Phys Chem 16:11381
33. Prajapati CS, Kushwaha A, Sahay PP (2013) Influence of Fe doping on the structural, optical and acetone sensing properties of sprayed ZnO thin films. Mater Res Bull 48:2687–2695
34. Pramod NG, Pandey SN, Sahay PP (2013) Sn-doped In2O3 nanocrystalline thin films deposited by spray pyrolysis: microstructural, optical, electrical, and formaldehyde-sensing characteristics. J Therm Spray Technol 22:1035–1043
35. Bougrine A, Addou M, Kachouane A, Bérnède JC, Morsli M (2005) Effect of tin incorporation on physicochemical properties of ZnO films prepared by spray pyrolysis. Mater Chem Phys 91:247–252
36. Sahay PP, Nath RK (2008) Al-doped ZnO thin films as methanol sensors. Sens Actuators B Chem 134:654–659
37. Raoufi D, Raoufi T (2009) The effect of heat treatment on the physical properties of sol-gel derived ZnO thin films. Appl Surf Sci 255:5812–5817
38. Chou TP, Zhang Q, Fryxell GE, Cao GZ (2007) Hierarchically structured ZnO film for dye sensitized solar cells with enhanced energy conversion efficiency. Adv Mater 19:2588–2592
39. Bhati VS, Ranwa S, Fanetti M, Valant M, Kumar M (2018) Efficient hydrogen sensor based on Ni-doped ZnO nanostructures by RF sputtering. Sens Actuators B 255:588–597

40. Iqbal J, Jan T, Ronghai Y (2013) Effect of Co doping on morphology, optical and magnetic properties of ZnO 1-D nanostructures. J Mater Science:Material Electonnics 24:4393–4398
41. Dey A (2018) Semiconductor metal oxide gas sensors: A review. Mater Sci Eng b 229:206–217
42. Zhang L, Zhao J, Zheng J, Li L, Zhu Z (2011) Shuttle-like ZnO nano/microrods: Facile synthesis, optical characterization and high formaldehyde sensing properties. Appl Surf Sci 258:711–718
43. Chu X, Chen T, Zhang W, Zheng B, Shui H (2009) Investigation on formaldehyde gas sensor with ZnO thick film prepared through microwave heating method. Sens Actuators B Chem 142:49–54
44. Lv P, Tang ZA, Yu J, Zhang FT, Wei GF, Huang ZX, Hu Y (2008) Study on a micro-gas sensor with SnO_2–NiO sensitive film for indoor formaldehyde detection. Sens Actuators B Chem 132:74–80
45. Wang J, Zhang P, Qi JQ, Yao P (2009) Silicon-based (2009) micro-gas sensors for detecting formaldehyde. J Sens Actuators B Chem 136:399–404
46. Zheng Y, Wang J, Yao P (2011) Formaldehyde sensing properties of electrospun NiO-doped SnO_2 nanofibers. Sens Actuators B Chem 156:723–730
47. Tian S, Ding X, Zeng D, Wu J, Zhang XieC (2013) A low temperature gas sensor based on Pd-functionalized mesoporous SnO_2 fibers for detecting trace formaldehyde. RSC Adv 3:11823